ELSEVIER

Journal of Molecular Catalysis A: Chemical 179 (2002) 221–231

JOURNAL OF MOLECULAR CATALYSIS A: CHEMICAL

www.elsevier.com/locate/molcata

Liquid phase oxidation of anthracene and *trans*-stilbene over modified mesoporous (MCM-41) molecular sieves☆

N. Srinivas, V. Radha Rani, S.J. Kulkarni*, K.V. Raghavan

Catalysis Group, Indian Institute of Chemical Technology, Hyderabad 500007, India

Received 23 February 2001; accepted 17 August 2001

Abstract

Transition metal ion incorporated MCM-41 has been found to be active for catalytic epoxidation of aromatic olefins (*trans*-stilbene) and oxidation of aromatic compound (anthracene). The Cr-MCM-41 catalyst was the best in comparison to the other isomorphously substituted MCM-41. *t*-Butylhydroperoxide (*t*-BHP) has shown better performance at around 80 °C in benzene as a solvent. The highest conversion of 79.3% of anthracene was observed with more than 90% selectivity of the product. Cr-MCM-41 could be used for the reaction without decrease in the catalytic activity.

Keywords: Transition metal-MCM-41; Oxidation; Anthracene; 9,10-Anthraquinone

1. Introduction

Porous inorganic materials, such as various zeolites which are crystalline aluminosilicates, have been particularly interesting because they possess uniform pores of various sizes and have been studied for their functions as molecular sieves, catalysts and supports [1]. But the micropore size present in certain zeolites, pose a problem of size restriction for the reactants, enabling reactions with larger molecules to proceed. The discovery of mesopore molecular sieves [2–4], facilitated to work with larger molecules also. Among them, mesoporous silicates/aluminosilicates with uniform hexagonal pores of about 30 Å (MCM-41) has been synthesized by hydrothermal process using a surfactant as an organic template [4,5]. Attempts to insert elements, such as Ti [6], Cr [7], Mn [8] or Fe [9] into the MCM-41 framework has been recently reported. Various oxidation reactions in liquid phase has been reported on heterogeneous catalyst [10–18].

Here, we report the oxidizing ability of MCM-41 which was synthesized hydrothermally and substituted with transition metal ions, both isomorphously and by impregnation method. The oxidation of anthracene and *trans*-stilbene was carried out in liquid phase. The oxidized product 9,10-anthraquinone, is widely used in the synthesis of dyes and during the large scale synthesis of hydrogen peroxide [19]. Conventionally, this was obtained by the oxidation of anthracene using chromic acid or vapor phase oxidation with air or by the reaction of phthalic anhydride and benzene in vapor phase [20].

2. Experimental

An aqueous solution of aluminum isopropoxide (0.38 g) and to it an aqueous solution of sodium hydroxide (0.3 g) was added in 50 ml beaker and

☆ IICT Communication No. 4593.

* Corresponding author. Tel.: +91-40-717-3874; fax: +91-40-717-3387.
E-mail address: sjkulkarni@iict.ap.nic.in (S.J. Kulkarni).

1381-1169/02/$ – see front matter
PII: S1381-1169(01)00328-4

stirred in hot conditions, till a clear solution was formed. Then 9.4 ml of tetraethyl ammonium hydroxide (TEAOH) and Ludox colloidal silica (9.26 g) were added drop wise while stirring at room temperature. Then hexadecyl tri-methylammonium bromide (10.55 g) was added slowly to the above solution. At the same time, an amount of transition metal precursor for 1 wt.% was dissolved in 5 g of water and then slowly added to the gel with stirring. The pH of the mixture was maintained at 11.0–11.5. Finally, the gel mixture was transferred into an autoclave and heated at 100 °C for 24 h. The solid product was recovered by filtration, washed with deionized water and dried in air. All the as-synthesized samples were calcined at 500 °C in air. Chromium impregnated MCM-41 was prepared by impregnating the calcined MCM-41 with an aqueous solution of a prescribed concentration of chromium nitrate, followed by evaporation of the solvent, drying at 120 °C for overnight and calcined at 420 °C for 4 h in air.

The reaction was carried out taking 35 ml of solvent benzene, 1 g of reactant and 1 g of catalyst in a round bottom flask. The reaction was carried out with stirring and under refluxing conditions for 24 h with reactant to *t*-butylhydroperoxide (*t*-BHP) molar ratio 1:4. The products were analyzed by HPLC and confirmed with authentic samples.

2.1. Measurements

The elemental composition of the resultant solid products was analyzed by ICP-MS. Powder XRD patterns of the as-synthesized and calcined products were recorded on a diffractometer with Cu Kα radiation at 0.045 step sized and 0.5 s step time over the range $0^\circ < 2\theta < 40^\circ$ which matched with the literature.

The specific surface area, A_{BET}, was determined from the linear part of BET plot ($P/P_0 = 0.05$–0.30). The SEM image of MCM-41 was observed at 15–150 kV, with 5000–10,000 magnification. The sample was coated with Au to prevent charge-up. The EDAX data was collected for each sample.

FT-IR measurements were performed on an FT-IR spectrophotometer using the KBr self-supported pellet technique. The pellets contained about 1% of finely powdered sample and were pressed at 4 ton cm^{-2}.

Diffuse reflectance UV–visible spectra were measured with a Perkin-Elmer 330 spectrophotometer equipped with a 60 mm Hitachi integrating sphere accessory. Pelleted samples were kept, and spectra were collected in the 200–800 nm wavelength range against an MCM-41 standard.

3. Results and discussion

The metal compositions of the solid products as determined by ICP-MS are in good agreement with the gel composition. The well-defined pattern of XRD in Fig. 1 is typical of MCM-41 as described by Kresge et al. [4,5]. All the three XRD reflections (1 0 0), (1 1 0), (2 0 0) are resolved and can be indexed to a hexagonal lattice. The synthesized MCM-41 was observed by SEM to directly confirm the presence of the hexagonal structure in the mesopore size. The BET surface area of the synthesized MCM-41 was 901 $m^2\,g^{-1}$. The physical properties of the MCM-41 obtained are listed in Table 1.

Fig. 2 shows the variation of the powder XRD patterns of the isomorphously substituted transition metal ion MCM-41 catalysts and BET surface area. The metal incorporated MCM-41 caused an appreciable decrease in the diffraction peaks at 2θ of 4–6°, together with the decrease in the surface area [21]. Particularly, the relative peak intensities of planes (1 1 0) and (2 0 0) at a 2θ of 4° decreased, which suggest a

Table 1
Physical properties of calcined MCM-41 and transition metal-MCM-41

Metal substituted	Metal ion (wt.%)	d(1 0 0) (Å)	a_0[a] (Å)	S_{BET} ($m^2\,g^{-1}$)
Na	1.0	43.00	49.7	901.0
Ti	∼1.0	38.48	44.4	865.0
V	0.38	37.63	43.5	840.0
Cr	0.46	37.83	43.6	838.5
Mn	0.70	38.55	44.5	870.0
Fe	0.69	37.39	43.2	820.0
Co	0.40	37.04	42.8	943.7
Ni	0.28	40.35	46.6	849.0
Cu	0.35	39.07	45.1	860.0
Zn	1.94	38.18	44.1	838.0
1% Cr		43.97	50.7	751.0
3% Cr		39.98	46.2	749.0
5% Cr		39.64	45.8	733.0

[a] The hexagonal unit-cell parameter (a_0) was calculated using the formula $a_0 = 2d(1\,0\,0)/\sqrt{3}$.

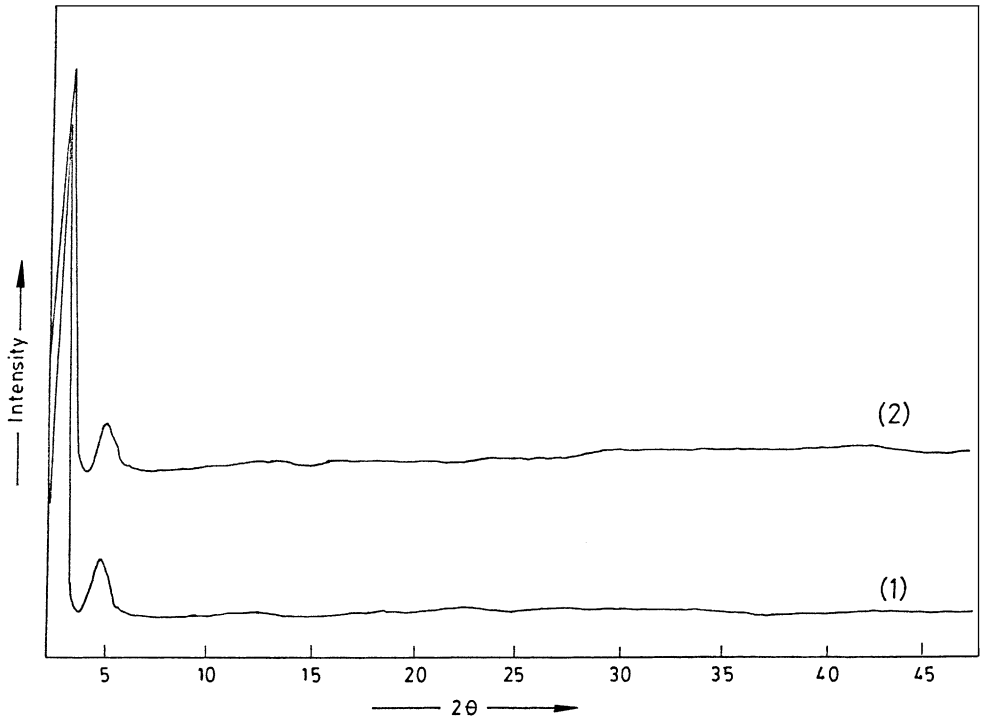

Fig. 1. XRD profiles of (1) MCM-41(calcined) and (2) MCM-41(as-synthesized).

decrease in the hexagonal regularity of the structure. Displacement of Al^{3+} with the transition metal ions, has been reported [22] to cause the imbalance in the polarity of the structure, which results in the destruction of the uniform hexagonal structure (Fig. 3).

The variation of the XRD patterns of the metal impregnated MCM-41 (Fig. 4) with the amount of the impregnation of the metal ion on the support did not cause appreciable change in the XRD pattern, and the $d(1\,0\,0)$ spacing slightly decreases with increasing Cr content, which is similar to Ga-MCM-41 [23]. The BET surface area decreased for 1 wt.% of Cr on the MCM-41 by $150\,m^2\,g^{-1}$, but the surface area did not decrease so much by increasing the amount of Cr impregnated on the MCM-41 and thus confirmed to preserve the hexagonal array and high surface area of MCM-41. It was reported that the unit-cell parameter (a_0) increases by 1–8 Å upon incorporation of transition metal into the framework of MCM-41 and by increasing the Cr content [24,25]. However, we observed the opposite as observed by Kevan and coworkers [7].

The IR spectra of calcined, dehydrated MCM-41 and transition metal ion incorporated MCM-41 are shown in Figs. 5 and 6. In all samples, an FT-IR band around $960\,cm^{-1}$ is observed, which is often assigned to a lattice defect and is correlated with the presence of tetrahedral framework ions as M–O–Si type [26–29]. This $960\,cm^{-1}$ band is also prominent in the FT-IR spectrum of calcined MCM-41. By carefully examining this band, it is seen that there is a slight red shift in metal incorporated samples. Recent work suggests [30] that this band can also be assigned to an Si–O vibration in an Si–OH group in siliceous MCM-41. If this is the case, it is reasonable to attribute the red shift in metal incorporated MCM-41 to the replacement of an OH group by O-metal ion.

Fig. 7 shows UV–visible spectra of as-synthesized and calcined, dehydrated Cr-MCM-41. The spectra of as-synthesized Cr-MCM-41 contains two typical bands of octahedral Cr(III) at 400 and 611 nm. They have been assigned to d–d transitions described as $^4A_{2g} \rightarrow {}^4T_{2g}$ and $^4A_{2g} \rightarrow {}^4T_{1g}$ transitions, respectively. The sharp shoulder at 467 nm in Figure 5 can

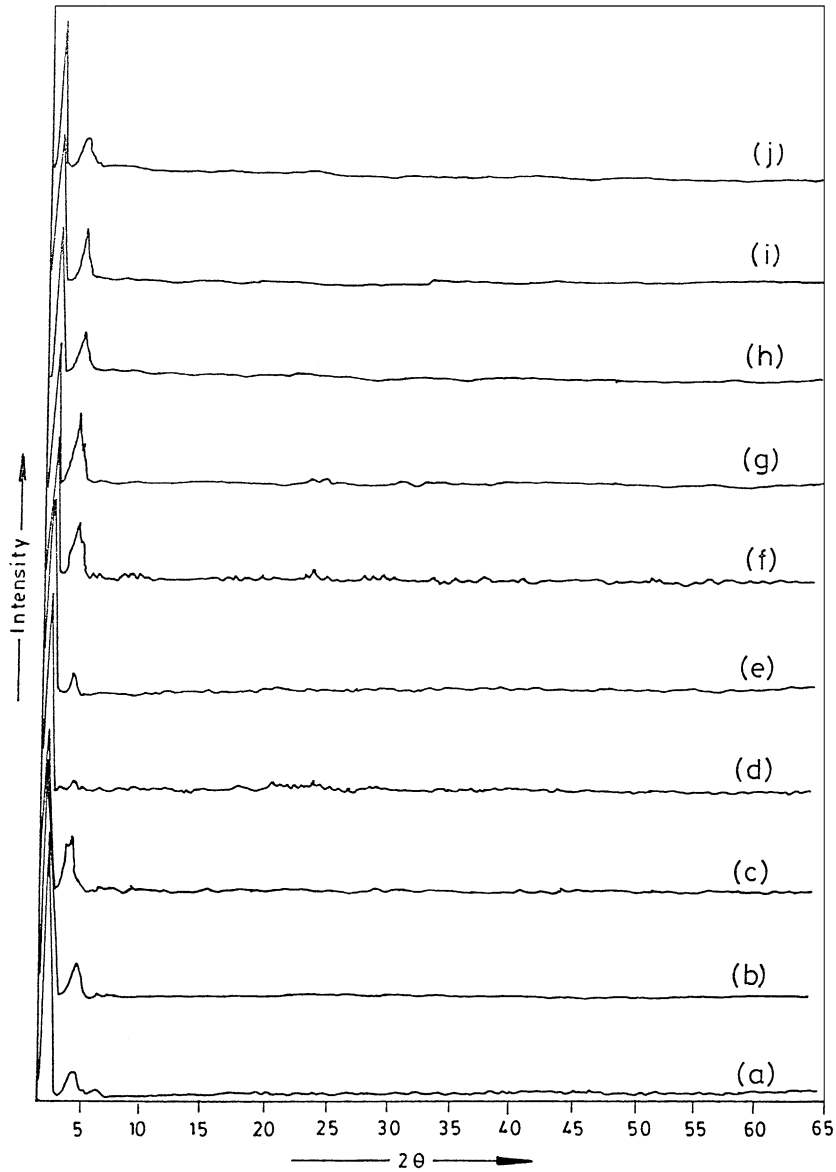

Fig. 2. XRD profiles of: (a) MCM-41, (b) Ti-MCM-41, (c) V-MCM-41, (d) Cr-MCM-41, (e) Mn-MCM-41, (f) Fe-MCM-41, (g) Co-MCM-41, (h) Ni-MCM-41, (i) Cu-MCM-41 and (j) Zn-MCM-41.

be assigned to a spin forbidden $A_{2g} \rightarrow^4 T_{2g}$ transition of six-coordinate under tetragonal distortion [7].

Fig. 8 shows the calcined Cr-MCM-41 electron spin resonance (ESR) spectra, wherein an intense signal around $g \sim 2.0053$ suggests the presence of trivalent chromium in octahedral coordination, while broad signal around $g \sim 1.978$ is characteristic of pentavalent chromium in tetrahedral or distorted tetrahedral coordination. This may be due to the partial oxidation of trivalent chromium during calcination.

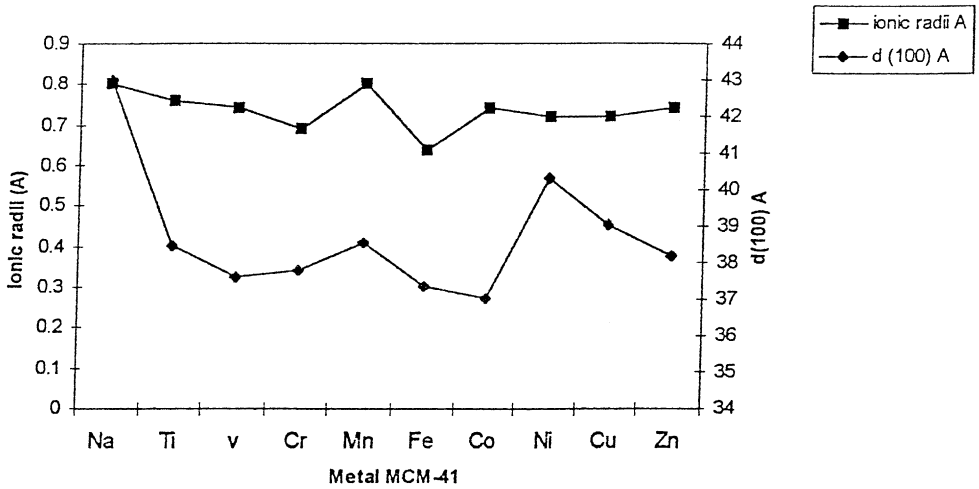

Fig. 3. Correlation of ionic radii and $d(1\,0\,0)$ spacing.

3.1. Oxidation of trans-stilbene

The activity of various catalysts was determined by carrying out epoxidation of *trans*-stilbene using benzene as a solvent and *t*-BHP as an oxidant under reflux condition (Table 2). MCM-41 itself showed very less activity with the yield of *trans*-stilbene-oxide being about 3.1 wt.% at 9.5 wt.% conversion. However, the conversion increased by about 8–10 folds on substituting transition metal ions in MCM-41 matrix. By incorporating 1 wt.% of the transition metal isomorphously, the activity followed the order

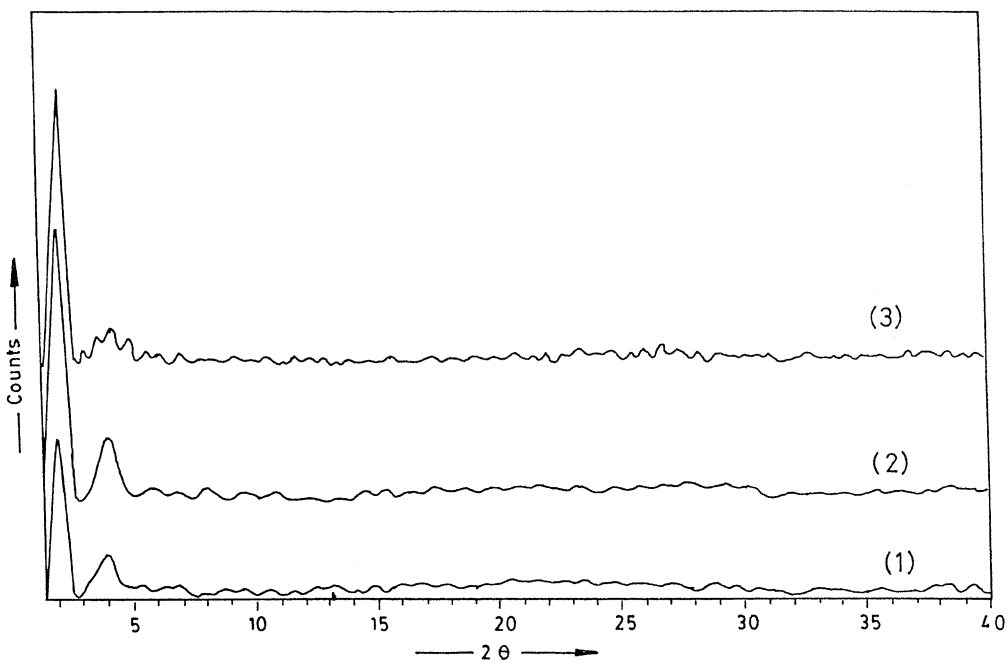

Fig. 4. XRD patterns of Cr impregnated MCM-41: (1) 1 wt.% Cr (2) 3 wt.% Cr and (3) 5 wt.% Cr.

Table 2
Liquid phase oxidation of *trans*-stilbene over modified MCM-41 catalysts[a]

S. No.	Catalyst	Conversion of *trans*-stilbene (wt.%)	Yield of products (wt.%)	
			trans-Stilbene oxide	Others
1	MCM-41	9.5	3.1	6.4
2	Cr-MCM-41	50.3	25.7	24.6
3	Fe-MCM-41	38.0	28.2	9.8
4	Co-MCM-41	43.7	27.9	15.8
5	Cr-MCM-41 (5 wt.% Cr)	59.6	34.2	25.4
6	FeZSM-5	11.2	4.6	6.6
7	CoZSM-5	16.3	1.9	14.4

[a] Reactant: *trans*-stilbene (1 g), reaction time: 20 h, solvent: benzene, reaction temperature: 80 °C, *trans*-stilbene:*t*-BHP = 1:2 molar, catalyst weight: 0.5 g.

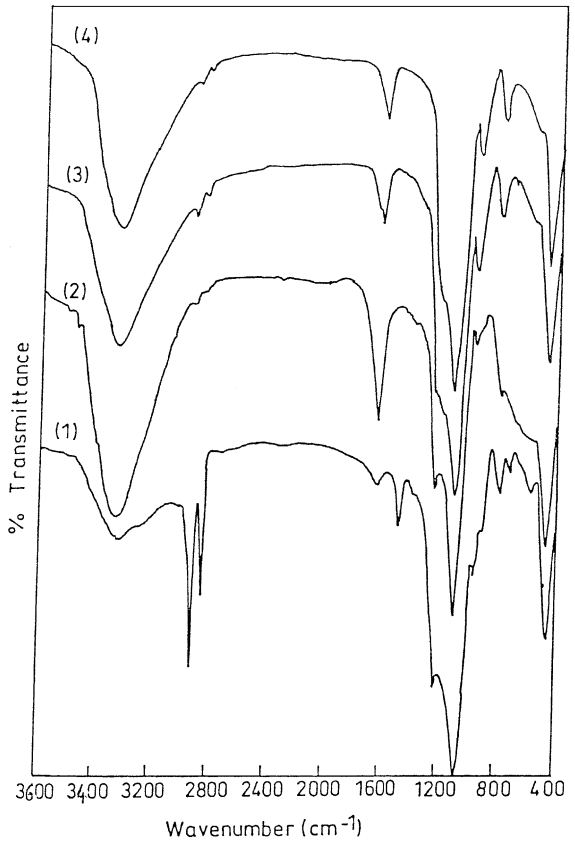

Fig. 5. IR spectra of: (1) MCM-41(as-synthesized), (2)MCM-41(calcined), (3) Ti-MCM-41, (4) V-MCM-41.

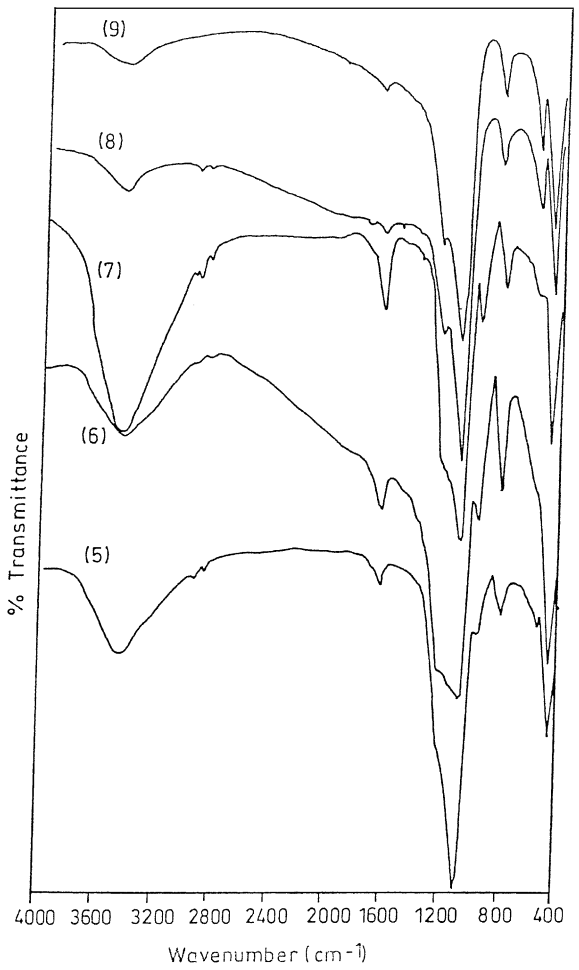

Fig. 6. IR spectra of (5) Cr-MCM-41, (6) Fe-MCM-41, (7) Co-MCM-41, (8) Cr-MCM-41 (impregnated), (9) Fe-MCM-41 (impregnated).

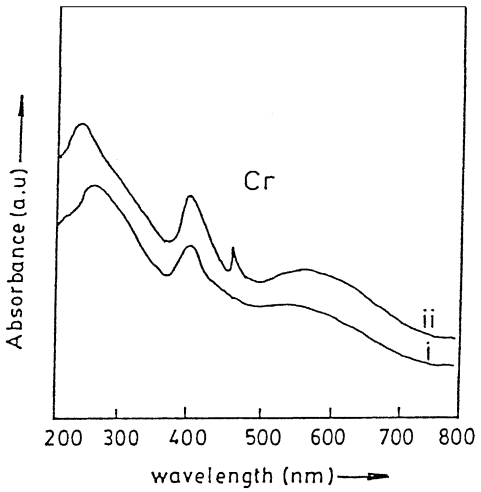

Fig. 7. Diffuse reflectance UV–visible (DRS) spectra of Cr-MCM-41: (i) as-synthesized, (ii) calcined.

Fe-MCM-41 ≤ Co-MCM-41 < Cr-MCM-41. The yields increased with the increase in wt.% from 1 to 5. In case of higher wt.% of metal ion, there are extra-framework metal ion metal oxide species may be present. The shape selectivity was more clearly confirmed on carrying out the reaction with FeZSM-5 (30) and CoZSM-5 (30), as both the catalysts gave very low yields of 4.6 and 1.9% *trans*-stilbene oxide under the identical reaction conditions. This could be a consequence of the steric constraints imposed by the smaller and three-dimensional pores present in HZSM-5 in comparison to the straight channels of MCM-41. Further, besides *trans*-stilbene oxide, the formation of benzaldehyde, benzoic acid, *t*-butoxybenzoate, 1,2-diphenylethandione, diphenyl acetaldehyde, and acetophenone could be the products. These side reactions including oxidation and carbon–carbon bond cleavage are not welcome and should be minimized. This shows that the transition metal modified MCM-41 molecular sieves are redox molecular sieves active in the oxidation reaction.

3.2. Oxidation of anthracene

3.2.1. Catalyst

The activity of various catalysts is shown in Fig. 9, where the catalytic run was performed with anthracene

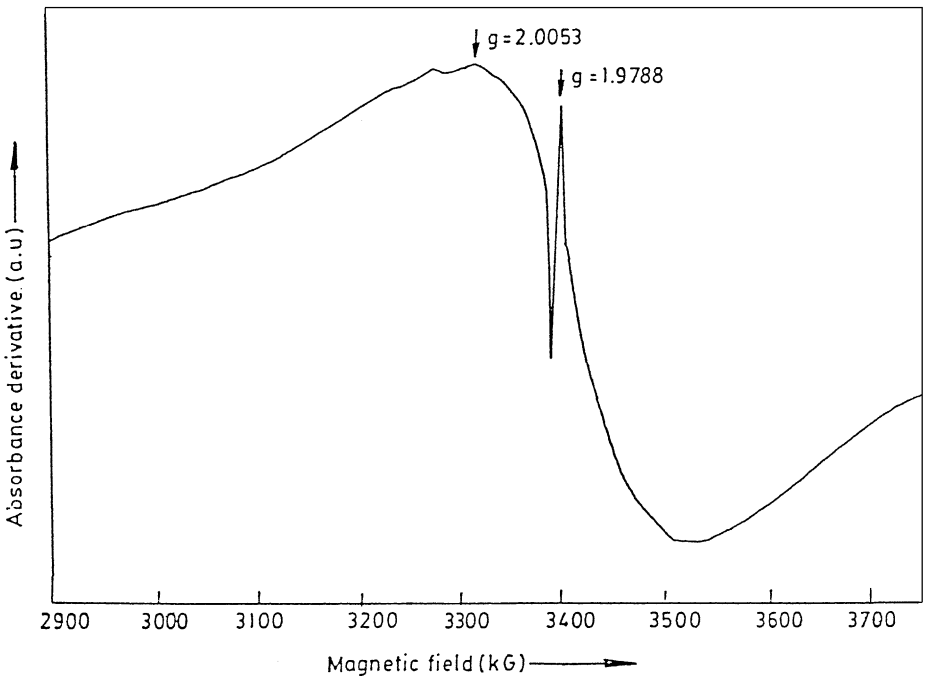

Fig. 8. ESR spectra of Cr-MCM-41.

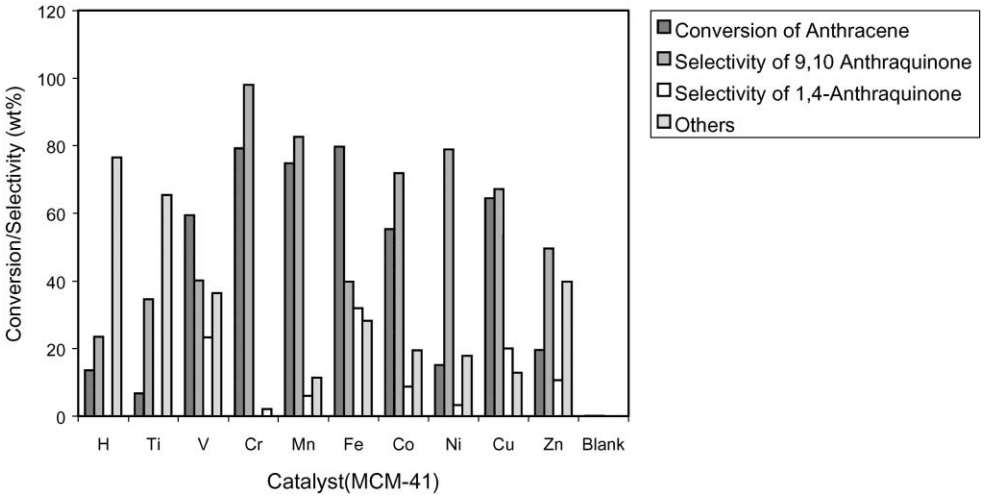

Fig. 9. Oxidation of anthracene over modified MCM-41 molecular sieves: variation of catalyst.

in benzene with 1:4 *tert*-butyl hydroperoxide (*t*-BHP) at 80 °C for 20 h. Without any catalyst, the yield of 9,10-anthraquinone was just in traces. On the other hand, the MCM-41 itself with no transition metal ion gave yields less than 10 wt.%.

The order of selectivity of 9,10-anthraquinone when the reaction was carried out over transition metal ion containing catalyst is Cr-MCM-41 > Mn-MCM-4 > Co-MCM-41 > Cu-MCM-41 >Fe-MCM-41 > V-MCM-41 > Ni-MCM-41 > Zn-MCM-41 > Ti-MCM-41. Thus it can be seen that the transition metal ions are, indeed, the active sites for oxidation. The effect of duration of the reaction of oxidation of anthracene is depicted in Table 3. The yield increased with increasing reaction time up to 20 h. Increasing the Cr wt.% from 1 to 5 (Table 4) by impregnation method, the conversion of anthracene improved, while yields showed slight variation. The reaction over CrHY (1 wt.%, Cr) resulted in drastic decrease of yields with decrease in selectivity.

3.2.2. Oxidant and solvent effect

Hydrogen peroxide (H_2O_2) and *t*-BHP were used as oxidants for catalytic oxidation of anthracene in benzene over Cr-MCM-41. The results are summarized in Table 5. The conversion was below 10% when H_2O_2 was used as the oxidant and benzene as a solvent. But as the solvents having higher dielectric constant (ε),

Table 3
Oxidation of anthracene: time on stream[a]

S. No.	TOS (h)	Conversion of anthracene (wt.%)	Liquid product selectivity (wt.%)		
			9,10-Anthraquinone	Others	TOF
1	3	12.8	91.4	8.6	557.14
2	6	24.3	84.0	16.0	485.7
3	9	31.7	92.1	7.9	463.5
4	12	40.4	93.8	6.2	
4	20	79.3	97.9	2.1	458.33

[a] Reactant: anthracene (0.25 g), catalyst: Cr-MCM-41, solvent: benzene (20 ml), anthracene:*t*-BHP = 1:4 molar, catalyst weight: 0.25 g.

Table 4
Oxidation of anthracene: metal % variation[a]

S. No.	Catalyst	Conversion of anthracene (wt.%)	Liquid product distribution (wt.%)		
			9,10-Anthraquinone	1,4-Anthraquinone	Others
1	Cr-MCM-41 (isomorphous)	79.3	97.9	–	2.1
2	Cr-MCM-41 (1 wt.% Cr)	95.2	93.3	–	6.7
3	Cr-MCM-41 (3 wt.% Cr)	96.2	97.1	–	2.9
4	Cr-MCM-41 (5 wt.% Cr)	91.5	96.4	1.1	2.5
5	CrHY (1 wt.% Cr)	34.6	68.8	18.2	13.0

[a] Reactant: anthracene (0.25 g), reaction time: 20 h, solvent: benzene (20 ml) anthracene:*t*-BHP = 1:4 molar, catalyst weight: 0.25 g.

Table 5
Oxidation of anthracene: variation of solvent and oxidant[a]

S. No.	Solvent	Oxidant	Conversion of anthracene (wt.%)	Liquid product selectivity (wt.%)		
				9,10-Anthraquinone	1,4-Anthraquinone	Others
1	Benzene	*t*-BHP	79.3	97.9	–	2.1
2	Benzene	H_2O_2	3.7	40.5	–	59.5
3	Toluene	*t*-BHP	46.5	83.9	–	16.1
4	Toluene	H_2O_2	23.9	44.8	14.2	41.0
5	THF	*t*-BHP	26.4	40.5	38.3	21.2
6	THF	H_2O_2	38.2	50.5	35.4	14.1

[a] Reactant: anthracene (0.25 g), catalyst: Cr-MCM-41, reaction time: 20 h, anthracene:oxidant = 1:4 molar, catalyst weight: 0.25 g.

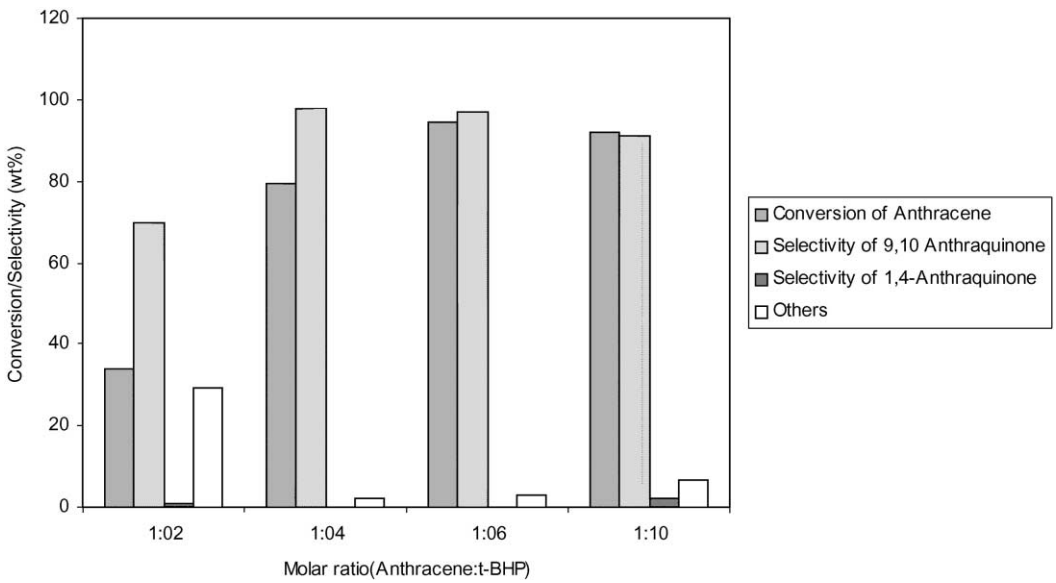

Fig. 10. Oxidation of anthracene: molar ratio variation.

Table 6
Oxidation of anthracene: molar ratio variation[a]

S. No.	Molar ratio	Conversion of anthracene (wt.%)	Liquid product distribution (wt.%)		
			9,10-Anthraquinone	1,4-Anthraquinone	Others
1	1:2	34.0	69.7	0.9	29.4
2	1:4	79.3	97.9	–	2.1
3	1:6	94.6	97.1	–	2.9
4	1:10	92.0	91.3	2.2	6.5

[a] Reactant: anthracene (0.25 g), reaction time: 20 h, solvent: benzene (20 ml), anthracene:*t*-BHP = 1:4 molar.

toluene ($\varepsilon = 2.38$) or THF ($\varepsilon = 7.58$) in comparison to benzene ($\varepsilon = 2.28$) was used and higher yields were obtained.

When *t*-BHP was used as the oxidant in the reaction system, the yields increased with the decreasing dielectric constant. As in apolar aprotic solvents of lower dielectric constant, the solute–solvent interaction decreases. So, in order to reduce the role of solvent, benzene was used as the solvent for the oxidation of anthracene with *t*-BHP. Further, Mokaya and Jones [26] reported the catalytic reactivity of transition-metal substituted MCM-41 for the benzene hydroxylation to phenol reaction. With the intention to verify, if benzene hydroxylation is competing with the anthracene oxidation, the same reaction was carried out without the reactant. However, no conversion of benzene was observed indicating that the catalyst is not very efficient for the benzene hydroxylation under the present reaction conditions.

3.2.3. Molar ratio variation

As the molar ratio of anthracene to *t*-BHP was varied from 1:2 to 1:10 (Fig. 10) for the oxidation of anthracene, it was observed that while increasing the *t*-BHP concentration, the yield of 9,10-anthraquinone increased with the conversion of anthracene being >90% (Table 6). Although as per stoichiometry, 1:2 ratio of oxidant is sufficient, but the requirement of higher ratio can be assigned to the non-selective thermal decomposition of the peroxide [31].

3.2.4. Recycle use of catalyst

One of the essential advantages in the use of solid catalyst in the liquid phase reaction is the easy separation of the catalyst from the solution containing reactants and products. The repeated use of the catalyst was indeed carried out at 80 °C. The first run gave 97.9% selectivity of 9,10-anthraquinone at 79.5% conversion of anthracene, after the 24 h reaction. Subsequently, the catalyst used was collected by filtration, dried at ambient temperature and activated at 400 °C for 4 h, then reused again in the second reaction. The same procedure was repeated for four times and the results are summarized in Table 7. The yields were essentially constant within an experimental error, indicating that the Cr-MCM-41 could be used repeatedly.

There remains an unsolved possibility that the Cr ions supported on the MCM-41 would dissolve in the solution during the reaction and the resulting Cr ions in the solution might be active for the oxidation

Table 7
Oxidation of anthracene: reusability of catalyst[a]

S. No.	Run	Conversion of anthracene (wt.%)	Liquid product distribution (wt.%)		
			9,10-Anthraquinone	1,4-Anthraquinone	Others
1	1	79.5	97.9	–	2.1
2	2	79.3	97.9	–	2.1
3	3	79.3	87.3	–	12.7
4	4	75.3	98.7	–	1.3

[a] Reactant: anthracene (0.25 g), catalyst: Cr-MCM-41, reaction time: 20 h, solvent: benzene (20 ml), anthracene:*t*-BHP = 1:4 molar, catalyst weight: 0.25 g.

reaction. The reaction was performed to investigate this possibility, in which the usual reaction was carried out at 80 °C for 3 h and then the catalyst was removed by filtration under hot condition. The yield of 9,10-anthraquinone was 11.7 wt.%. The reaction was continued for another 20 h with the remaining filtrate. The yield value was almost the same as after 3 h reaction. It concludes that the active sites for oxidation are the Cr ions in MCM-41 and they can be used repeatedly.

4. Conclusions

1. 9,10-Anthraquinone was obtained from anthracene using Cr-MCM-41 catalyst and *t*-BHP in liquid phase. The selectivity was 97.9% at 79.5% conversion.
2. The other transition metal ion modified MCM-41 are also active in the liquid phase oxidation of anthracene. Cr-MCM-41 is found to be the best catalyst.
3. *t*-BHP is the best oxidant.

Acknowledgements

We are thankful to Dr. D. Vijaykumar for his help in HPLC analysis and Department of Science and Technology of New Delhi for financial help (DST-SP/S1/H07/97).

References

[1] R.M. Barrer, J. Chem. Soc., Chem. Commun. (1948) 2158.
[2] M.E. Davis, C. Saldarriaga, C. Montes, J. Garces, C. Crowder, Nature 698 (1988) 331.
[3] M. Estermann, L.B. Mc Cusker, C. Baerlocher, A. Merrouche, H. Kessler, Nature 320 (1991) 352.
[4] C.T. Kresge, M.E. Leonowicz, W.J. Roth, J.C. Vartuli, J.S. Beck, Nature 359 (1992) 680.
[5] J.S. Beck, J.C. Vartuli, W.J. Roth, M.E. Leonovicz, C.T. Kresge, K.D. Schmitt, C.T.W. Chu, D.H. Olson, E.W. Sheppard, S.B. Mc Cullen, J.B. Higgins, J.L. Schlenker, J. Am. Chem. Soc. 114 (1992) 10834.
[6] T. Blasco, A. Corma, M.T. Navarro, J.P. Pariente, J. Catal. 156 (1995) 65.
[7] Z. Zhu, Z. Chang, L. Kevan, J. Phys. Chem. B 103 (1999) 2680.
[8] D. Zhao, D. Goldfarb, J. Chem. Soc., Chem. Commun. (1995) 875.
[9] Z.Y. Yuan, S.Q. Liu, T.H. Chen, J.Z. Wang, H.X. Li, J. Chem. Soc., Chem. Commun. (1995) 973.
[10] T. Maschmeyer, F. Rey, G. Sanker, J.M. Thomas, Nature 378 (1995) 159.
[11] A. Corma, P. Esteve, A. Martinez, S. Valencia, J. Catal. 152 (1995) 18.
[12] T. Blasco, A. Corma, M.T. Navarro, J. Perez Pariente, J. Catal. 156 (1995) 65.
[13] J.S. Reddy, R. Kumar, J. Catal. 130 (1991) 440.
[14] W. Zhang, M. Froba, J. Wang, P.T. Tanev, T.J. Pinnavia, J. Am. Chem. Soc. 118 (1996) 9164.
[15] R.C. Oldroyd, J.M. Thomas, T. Maschmeyer, P.A. MacFaul, D.W. Snelgrove, K.U. Ingold, D.D.M. Wayner, Angew. Chem. Int. Ed. Eng. 35 (1996) 2787.
[16] W.A. Carvalho, P.B. Varaldo, M. Wallau, U. Schuchardt, Zeolites 18 (1997) 408.
[17] S. Gontier, A. Tuel, J. Catal. 157 (1995) 124.
[18] A.R. Tian, W. Tong, J.Y. Wang, N.G. Duan, V.V. Krishnan, S.L. Suib, Science 276 (1997) 926.
[19] N. Srinivas, V. Radha Rani, M. Radha Kishan, S.J. Kulkarni, K.V. Raghavan, J. Mol. Catal. A 172 (2001) 187.
[20] Ullmann's Encyclopedia of Industrial Chemistry, Vol. 2, VCH, Weinheim, 1985, pp. 347–354.
[21] J. Okamura, S. Nishiyama, S. Tsuruya, M. Masai, J. Mol. Catal. 135 (1998) 133.
[22] Z. Luan, H. He, W. Zhou, C.F. Cheng, J. Klinowski, J. Chem. Soc., Faraday Trans. 91 (1995) 2955.
[23] C. Cheng, H. He, W. Zhou, J. Klinowski, J. Goncalves, L. Gladden, J. Phys. Chem. 100 (1996) 390.
[24] N. Ulagappan, C.N.R. Rao, J. Chem. Soc., Chem. Commun. (1996) 1047.
[25] W. Zhang, J. Wang, P.T. Tanev, T.J. Pinnavaia, J. Chem. Soc., Chem. Commun. (1996) 979.
[26] R. Mokaya, W. Jones, J. Chem. Soc., Chem. Commun. (1996) 981.
[27] P.T. Tanev, T.J. Pinnavaia, Science 267 (1995) 865.
[28] P.T. Tanev, M. Chibwe, T.J. Pinnavaia, Nature 368 (1994) 321.
[29] T. Chapus, A. Tuel, Y. Taarit, C. Naccache, Zeolites 14 (1994) 349.
[30] S. Schwarz, D.R. Corbin, A.J. Vega, in: R.F. Lobo, J.S. Beck, S.L. Suib, D.R. Corbin, M.E. Davis, L.E. Iton, S.I. Zones (Eds.), Materials Research Society Symposium Proceedings, Vol. 431, Materials Research Society, Pittsburg, PA, 1996, p. 137.
[31] M. Yonemitsu, Y. Tanaka, M. Iwamoto, J. Catal. 178 (1998) 207.